

Figure S1. *mut-5* affects assembly of several non-DSR facultative heterochromatin islands but not constitutive heterochromatin, related to Figure 1.

(A) Non-DSR heterochromatin islands that are remodeled in response to meiotic induction triggered by nitrogen starvation. H3K9me2 distribution at individual islands was determined by ChIP-chip from (Zofall et al., 2012). Note that islands 3, 7, 13, 14, 15 and 19 but not island 21 show severe reduction in H3K9me2 upon nitrogen starvation. (B) Heterochromatin at the mating type locus (*mat*) and pericentromeric repeats (*dg660*) is preserved in *mut-5* cells. Conventional ChIP analyses with average enrichments and standard deviation of experimental replicates are shown. (C) Loss of H3K9me2 at several non-DSR islands in *mut-5* cells. The distribution of H3K9me at the indicated islands in *epe1Δ* and *epe1Δ mut-5* strains was determined by microarray analysis.

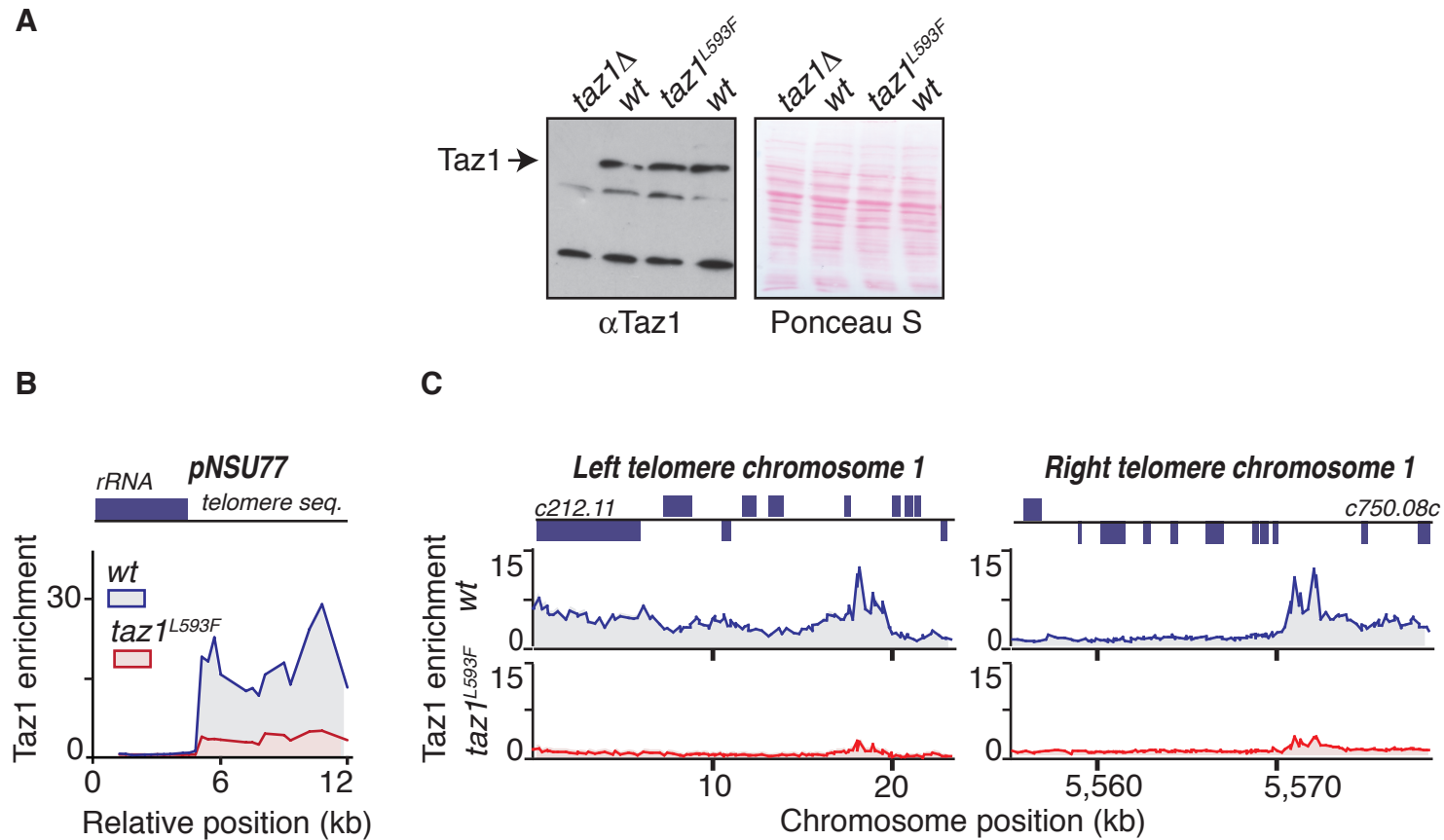


Figure S2. The Taz1^{L593F} substitution in the Myb domain interferes with Taz1 binding to telomeres, related to Figure 2.

(A) Expression of wild type and Taz1^{L593F} protein. Anti-Taz1 antibody was used to detect the wild type and mutant protein. The Ponceau stained protein loading control is shown. (B and C) Taz1 distribution in wild type and *taz1^{L593F}* cells at the telomere and subtelomere regions was determined by ChIP-chip using probes derived from the telomere plasmid pNSU77 containing *rDNA* and telomeric sequences (B), and the left and right telomere of chromosome 1 (C). The positions of ORFs are indicated above the panels. ChIP was performed using anti-Taz1 antibody. Relative position in (B) refers to the numbering along the cloned sequence in pNSU77.

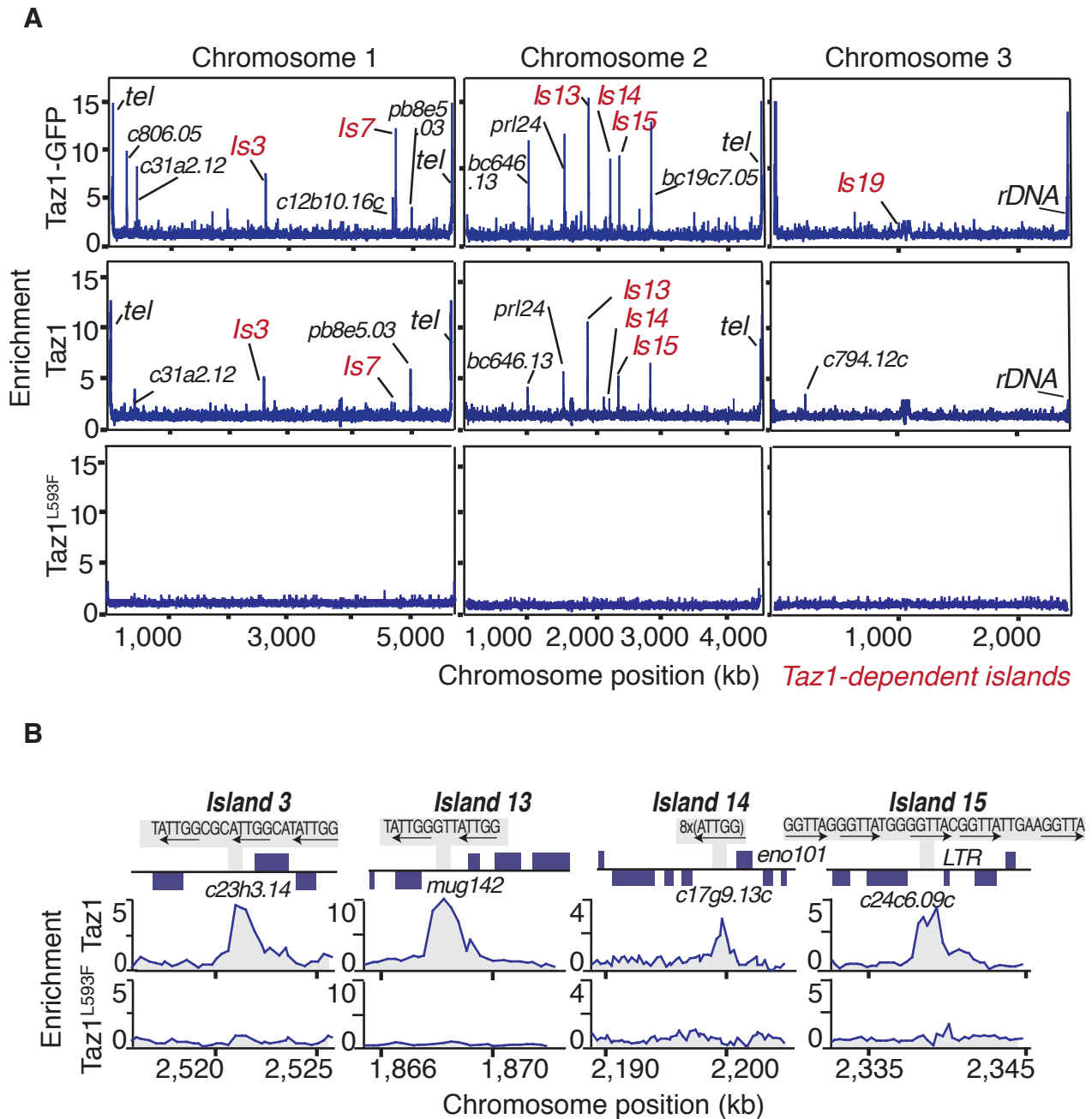


Figure S3. The Taz1^{L593F} mutation in the Myb domain impairs Taz1 localization at heterochromatin islands, related to Figure 3.

ChIP-chip was used to assay Taz1, Taz1-GFP and Taz1^{L593F} localization along chromosomes (A), and at Taz1-dependent heterochromatin islands (B). The positions of ORFs and telomere-like repeats are indicated.

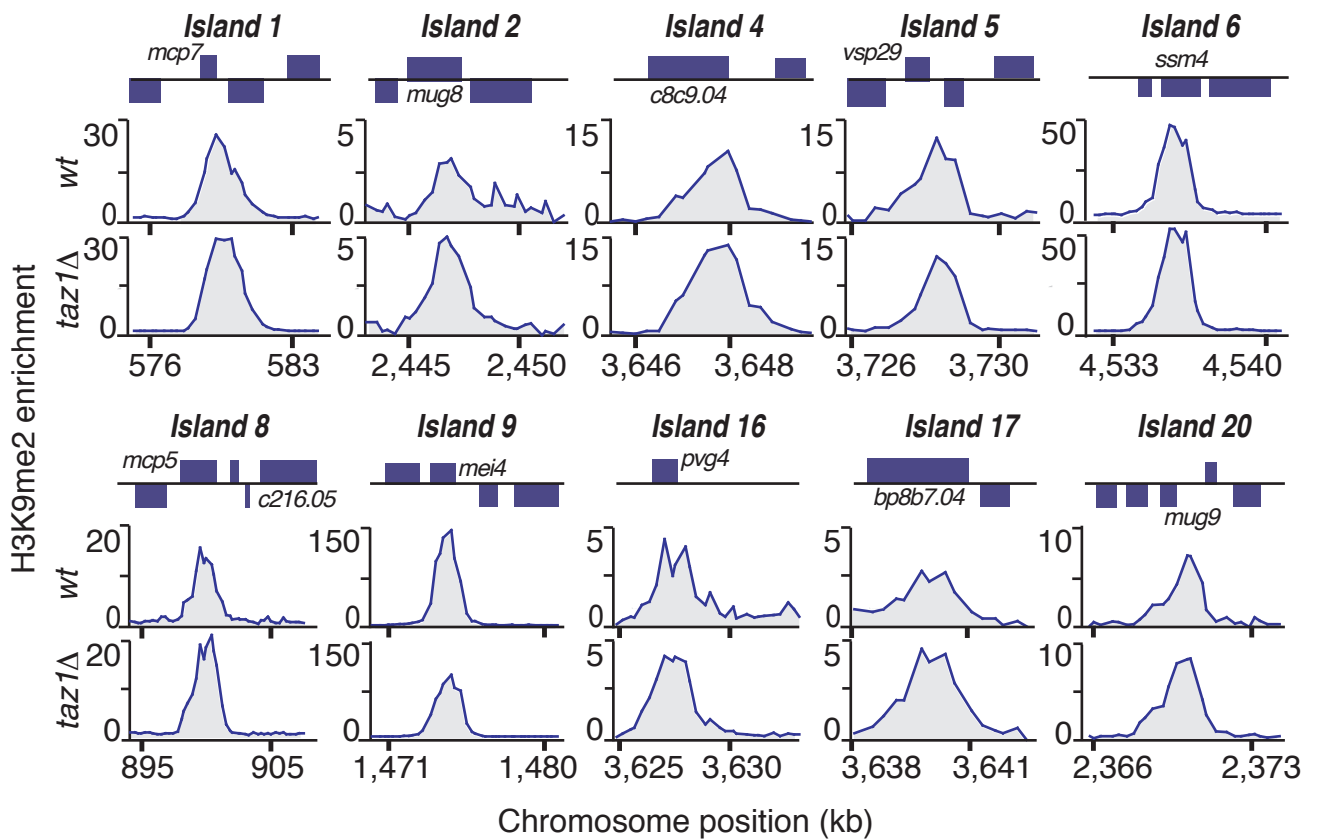


Figure S4. *Taz1* does not affect H3K9me at DSR islands, related to Figure 4.

ChIP-chip was used to compare H3K9me2 levels in DSR-containing heterochromatin islands in wild type and *taz1Δ* cells. Wild type H3K9me2 microarray data are from (Zofall et al., 2012). The positions of ORFs are indicated above the panels.

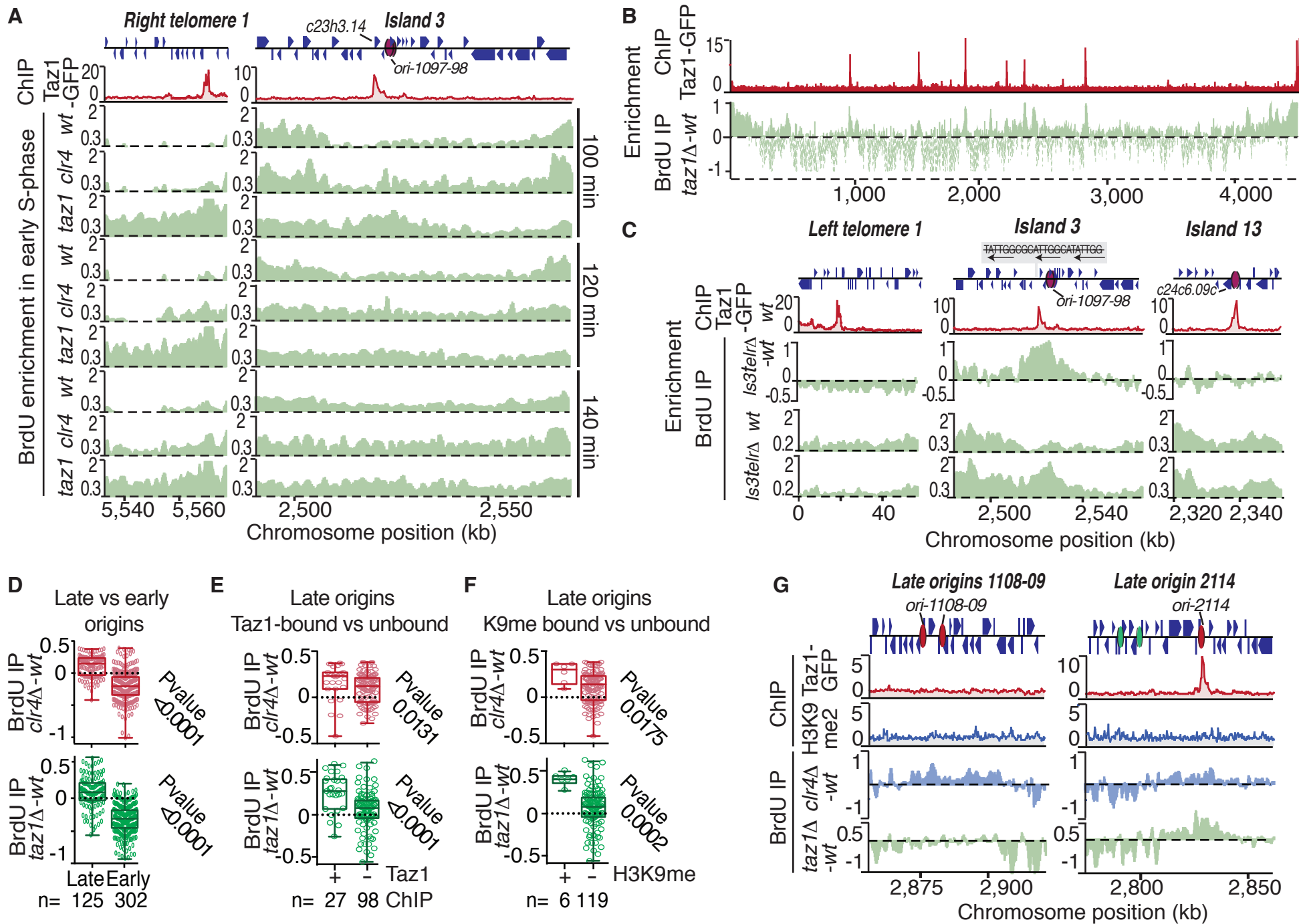


Figure S5

Figure S5. Heterochromatin factors affect the timing of replication initiation, related to Figure 6.

(A) ChIP-chip analysis of BrdU incorporation in the indicated strains. Mutant *cdc25-22* cells arrested at the G2/M boundary were released into the cell cycle in medium supplemented with HU and BrdU. Samples were collected at the indicated time points and used to perform BrdU ChIP-chip analysis. (B, C) Taz1 regulates the replication activity of proximal late origins. (B) Enhanced BrdU incorporation at Taz1-bound loci in *taz1Δ* cells. The distribution of Taz1-GFP along chromosome 2 (top panel) is shown in alignment with BrdU incorporation in early S-phase *taz1Δ* cells (lower panel). (C) Deletion of the Taz1 binding sequences at island 3 stimulates the activity of late replicating origins 1097/98 (indicated by red ovals), but does not affect the replication of subtelomeric or island 13 DNA. (D, E, F) Median difference distribution of BrdU IP signals between the indicated mutant and wild type at early and late replication origins (D), or at late replicating origins grouped according their association with Taz1 (E), or with heterochromatin islands (F). Bars represent the interquartile distribution ranges and the dividing lines represent the median values; n, number of origins in each group. Whiskers indicate minimal and maximal distribution values. The distribution plotted corresponds to the 120 minute BrdU IP time point in panel A. See Supplementary Methods for more details. (G) The replication activity (BrdU enrichment) of origins that are not associated with heterochromatin islands was determined for *clr4Δ* and *taz1Δ*. The mutant and wild type BrdU ChIP-chip profiles are shown in the bottom two panels. Taz1-GFP and H3K9me2 distributions are shown in the top panels. The ORF positions (blue), late origins (red ovals) and early replicating origins (green ovals) are indicated at the top. H3K9me2 analysis is based on data published in Zofall et al 2012.

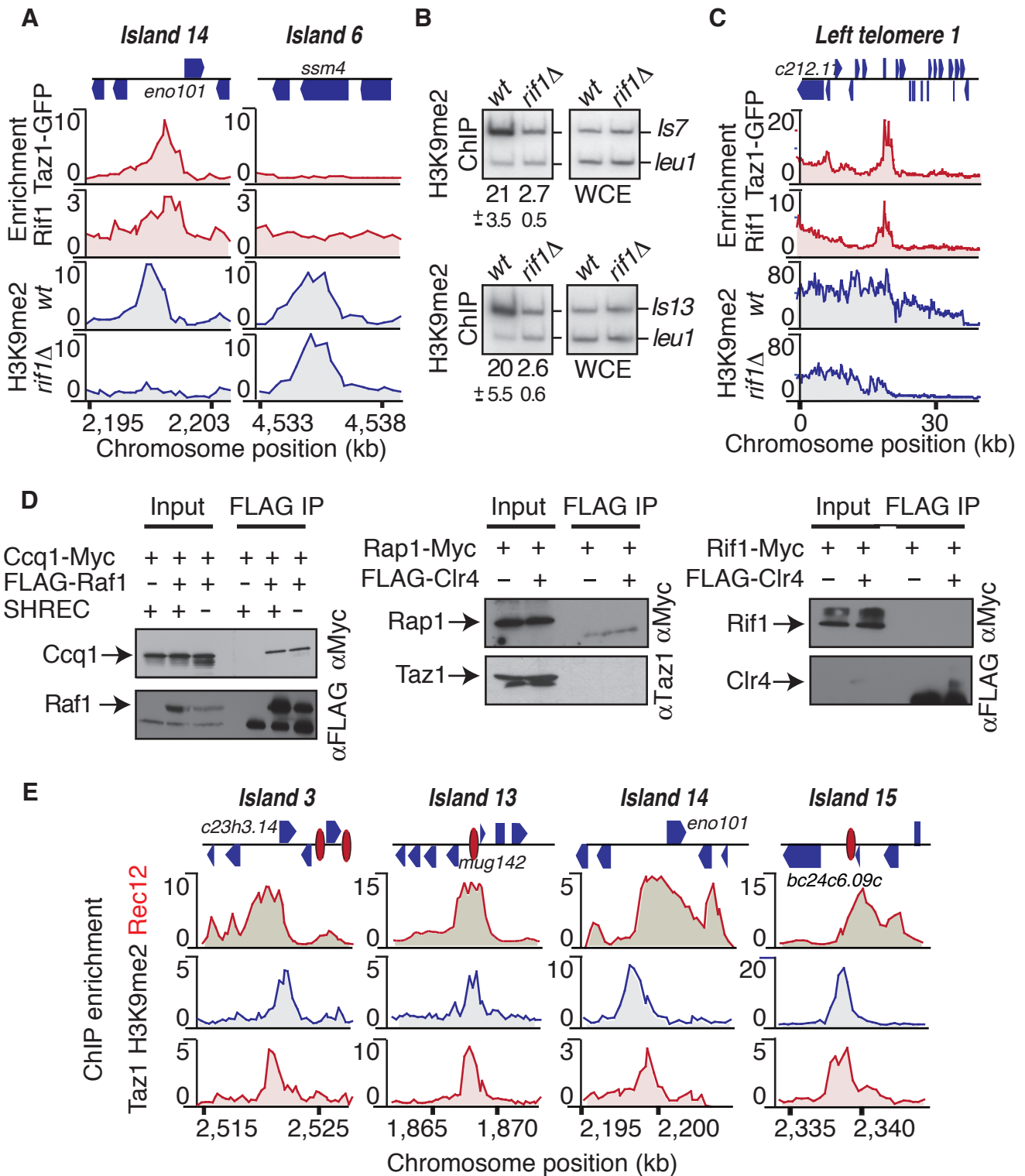


Figure S6. Rif1 selectively promotes heterochromatin assembly, related to Figure 7.

(A) Rif1 localizes to and promotes H3K9me at Taz1-dependent heterochromatin island 14 (left panel), but does not affect DSR island 6 (right panel). (B) Conventional H3K9me ChIP analysis at Taz1-dependent islands. The average enrichments and standard deviations of two measurements are indicated. (C) Rif1 is required for H3K9me at a subtelomeric heterochromatin domain. Rif1 and H3K9me2 levels were determined by ChIP-chip. (D) Association of Shelterin components with ClrC was determined by co-IP analysis. Ccq1, but not Taz1, Rap1 or Rif1 was present in the ClrC co-purified protein fraction. Note that Ccq1 associates with Raf1 in cells lacking the SHREC subunit Clr3 (left panel). (E) Taz1-dependent heterochromatin islands map to sites of meiotic double strand DNA breaks. Rec12-DNA adducts isolated from cells undergoing synchronized meiosis (top panel) as well as H3K9me2 and Taz1 localization in vegetative cells are plotted for the indicated Taz1-dependent islands. The ORF positions and late replicating origins (red ovals) are indicated at the top. H3K9me2 microarray data from (Zofall et al., 2012) was used.

List of Supplemental Tables

Table S1. List of Taz1-dependent heterochromatin islands containing late replication origins, related to Figure 3

Table S2. Strains used in this study, related to Experimental Procedures

Table S3. Primers used to construct strains with deleted telomere repeat-like sequence at island 3 or island 15, related to Experimental Procedures

Table S4. Primers used in this study, related to Experimental Procedures

Supplementary Experimental Procedures

Deletion of telomere repeat-like sequences at islands 3 and 15. A two-step strategy was used to construct a “clean” deletion of Taz1 binding sequences at island 3 and island 15. First, *ura4⁺* was inserted at the site of the deletion by homologous recombination as described in Bahler et al., 1998. Subsequently the *ura4⁺* marker was replaced by homologous integration of a DNA fragment that overlaps the *ura4⁺* insertion site and contains the deletion of Taz1 binding sequences. Oligonucleotides and the final sequence after deletion of Taz1 binding sites can be found in Table S3.

ChIP and ChIP-chip. ChIP-chip was performed essentially as previously described (Cam et al., 2007; Zofall et al., 2012). Exponentially growing *S. pombe* cultures were treated with 3% paraformaldehyde for 30 minutes. PBS-washed cells were subjected to additional crosslinking as required with 10 mM dimethyl adipimidate (Sigma-Aldrich) for 45 min at room temperature. After re-suspension in lysis buffer (50mM HEPES/KOH pH7.5, 140 mM NaCl, 1% Triton X100 and 0.1% sodium deoxycholate) supplemented with Roche Complete protease inhibitors, crosslinked cells were lysed by bead-beating using a Biospec Mini-Beadbeater-16 and the extracted chromatin was sheared by sonication to 0.5-1 kb fragments. Chromatin was cleared by centrifugation at 1,500xg, pre-incubated with protein A or G agarose and immunoprecipitated by overnight incubation with appropriate antibody (1-3 μ g). The immunopurified chromatin bound to Protein A or G was washed with the following solutions: 2x with lysis buffer (NaCl was adjusted to 500mM for the second wash), wash buffer (10mM Tris/HCl pH 8, 250mM LiCl, 0.5% NP40, 0.5% sodium deoxycholate and 1mM EDTA) and TE buffer. Immunoprecipitated chromatin was eluted by incubating in TE supplemented with 1% SDS for 30 minutes at 65 °C twice and pooling the eluates. Recovered chromatin was reverse crosslinked for 16 hours at 65 °C and the DNA was purified using a Qiaquick PCR purification kit (Qiagen) after treatment with 5 μ g of RNase A and 40 μ g of Protease K (30 minutes at 37 °C each). Immunoprecipitated and input DNA were analyzed by quantitative duplex PCR using the primers listed in Table S4. PCR products were resolved on a 4% PAGE gel, visualized and quantified by phosphorimaging (Typhoon FLA 9500, GE Healthcare). Relative enrichment values were calculated as a ratio of the intensities of PCR products from the heterochromatic and control loci in the ChIP DNA sample, normalized to the ratio obtained from the input DNA reaction. Alternatively, DNA was

amplified by a two step random-primed PCR for microarray analysis. First, immunoprecipitated and input DNA were copied by T7 DNA polymerase (USB) in two cycles primed by a primer comprised of specific sequences and random nonamers (Primer A; Supplementary Table S4). The DNA was cleaned and concentrated using an Amicon Ultra 30K (Millipore) filter spin column. Aminoallyl-dUTP was incorporated into DNA by PCR amplification using oligonucleotide Primer B matching the 5' end specific sequence of Primer A (Table S4). The modified DNA was purified using the Qiaquick PCR purification kit (Qiagen), vacuum evaporated and dissolved in 5 μ l of 2x coupling buffer (0.1M Na HCO₃), combined with an equal volume of 10mg/ml of Cy5 or Cy3 dissolved in DMSO, and Qiaquick-purified after conjugation at room temperature for >2 hours. Equal amounts of Cy3-labeled input DNA and Cy5-labeled immunoprecipitated DNA were hybridized to an Agilent 4x44K custom 60-mer oligonucleotide array, and slides were washed and prepared for scanning on the Agilent SureScan Microarray Scanner according to Agilent's protocol. The Cy3 and Cy5 signals were extracted and processed using the Agilent Feature Extraction protocol ChIP_1105_Oct12. The Cy5/Cy3 ratio of LOWES normalized signals was used to calculate enrichment values, which were further processed by a three probe sliding window filter to reduce noise. Enrichment values larger than 2 were replaced by the average enrichment values of two neighbors unless the enrichment of one neighboring probe was also above 2. For the analysis of H3K9me2 ChIP-chip data, an additional filter that defines heterochromatin islands was applied; all probe enrichment values were set to a value of 1, unless they satisfied the definition of an island as a region of at least 4 consecutive probes exceeding an enrichment value of 2.

Replication assay. The replication assays were performed as described previously (Hayashi et al., 2007; Tazumi et al., 2012). *cdc25-22* cells carrying the herpes simplex virus thymidine kinase expression module *Pnmt1-TK* and the human nucleoside transporter module *Padh1-hENT* were grown in EMM minimal media at 26 °C. After reaching an optical density of 0.1-0.2, the G2/M block was initiated by incubating cells at 37 °C for 4 hours and 15 minutes. Cells were released from the G2/M block by lowering the temperature to 26 °C. The culture was supplemented with 10mM hydroxyurea and 200 μ M 5-bromo-2'-deoxyuridine at the time of release. Cell septation was monitored by microscopy to estimate the efficiency of cell-cycle

synchronization. At the time corresponding to early S-phase, 5×10^7 cells were collected and fixed with 0.1% sodium azide, washed with PBS and resuspended in lysis buffer (10mM Tris/HCl pH 8.0, 100 mM NaCl, 1mM EDTA, 2% Triton X100, and 1% SDS). The cell suspension was combined with phenol-chloroform and lysed by bead beating. DNA was recovered from the aqueous phase by ethanol precipitation and sonicated to 0.5-1 kb fragments before treatment with $2 \mu\text{g}$ of RNase A. DNA was recovered by ethanol precipitation after phenol-chloroform extraction. BrdU labeled DNA was immunoprecipitated with mouse anti-BrdU antibody (BD Pharmingen) immobilized to Dynal anti-mouse Ig magnetic beads (Invitrogen), and washed as in the ChIP procedure. Immunoprecipitated DNA was eluted from beads by incubation with 1% SDS at 65°C for 30 minutes and purified by treatment with $60 \mu\text{g}$ of Proteinase K at 50°C for 2 hours, followed by phenol-chloroform extraction and ethanol precipitation. Immunoprecipitated and input DNA were random-prime PCR amplified and analyzed on Agilent 4x44K microarrays as described for ChIP-chip. A sliding window filter was applied for noise reduction, and the enrichment data were smoothed using the unweighted sliding average method over intervals corresponding to the DNA fragment size after sonication ($\sim 1\text{kb}$).

Processing of BrdU microarray data for statistical analysis. The positions and naming of early and late replicating origins were based on Hayashi et al., 2007. Smoothed enrichment data were used to calculate median values of the BrdU enrichment differences between mutant and wild type samples over 3kb intervals centered on the replication origin position. Taz1-bound origins were defined as origins within 5 kb of Taz1-GFP binding peaks. Our analysis also included previously reported Taz1-bound origins (Tazumi et al., 2012); origins within 100kb of telomeres were excluded from analysis. The significance of the median difference between two groups of replication origins was determined using the unpaired t-test. Box plots extend from the 25th to the 75th percentiles, and the horizontal line indicates the median value. Whiskers indicate the maximal and minimal values of each data set.

Rec12 ChIP. A modified method for determining the distribution of Rec12-FLAG self-linked to double stranded DNA breaks was adopted from a previously published protocol (Cromie et al.,

2007). *pat1-114* haploid cells carrying the *rad50S* allele were grown in minimal EMM media at 25 °C to an optical density of 0.3-0.4. Cells were then transferred to minimal media lacking NH₄Cl and incubated for 18 hours at 25 °C. Synchronized meiosis was initiated by the addition of 0.5% NH₄Cl combined with a temperature shift to 36 °C. Cells harvested after 4 hours at 36 °C were washed with PBS, re-suspended in 10% trichloroacetic acid (TCA) and lysed by bead beating. TCA precipitated proteins were collected by centrifugation at 17,000xg and dissolved by boiling in 2% SDS. Before immunoprecipitation, the SDS was diluted to < 0.1% with IP buffer (30mM Tris/HCl pH 8.0, 300 mM NaCl, 2mM EDTA, 2% Triton X100 and 0.02% SDS) and the chromatin was fragmented by sonication. Chromatin immunoprecipitation and microarray analysis was performed as described for ChIP-chip.

Supplemental References

Bahler, J., Wu, J.Q., Longtine, M.S., Shah, N.G., McKenzie, A., Steever, A.B., Wach, A., Philippsen, P., and Pringle, J.R. (1998). Heterologous modules for efficient and versatile PCR-based gene targeting in *Schizosaccharomyces pombe*. *Yeast* 14, 943-951.

Cam, H.P., Noma, K.-i., Ebina, H., Levin, H.L., and Grewal, S.I.S. (2007). Host genome surveillance for retrotransposons by transposon-derived proteins. *Nature* 451, 431-436.

Cromie, G.A., Hyppa, R.W., Cam, H.P., Farah, J.A., Grewal, S.I., and Smith, G.R. (2007). A discrete class of intergenic DNA dictates meiotic DNA break hotspots in fission yeast. *PLoS Genet.* 3, 1496-1507.

Hayashi, M., Katou, Y., Itoh, T., Tazumi, A., Yamada, Y., Takahashi, T., Nakagawa, T., Shirahige, K., and Masukata, H. (2007). Genome-wide localization of pre-RC sites and identification of replication origins in fission yeast. *EMBO J.* 26, 1327-1339.

Tazumi, A., Fukuura, M., Nakato, R., Kishimoto, A., Takenaka, T., Ogawa, S., Song, J.-H., Takahashi, T.S., Nakagawa, T., Shirahige, K., *et al.* (2012). Telomere-binding protein Taz1 controls global replication timing through its localization near late replication origins in fission

yeast. *Genes Dev.* 26, 2050-2062.

Zofall, M., Yamanaka, S., Reyes-Turcu, F.E., Zhang, K., Rubin, C., and Grewal, S.I.S. (2012). RNA elimination machinery targeting meiotic mRNAs promotes facultative heterochromatin formation. *Science* 335, 96-100.